MODELLING OF HYDRODYNAMIC CAVITATION FOR TREATMENT OF WASTEWATER IN A VENTURI TUBE

Betti Bolló

Department of Fluid and Heat Engineering, University of Miskolc, 3515 Miskolc, Hungary
e-mail: aramzb@uni-miskolc.hu

ABSTRACT

Treatment of municipal effluents has long been a challenge for modern technologies combining high effectiveness of degradation of pollutants with low costs of the process. Hydrodynamic cavitation is a promising application in wastewater treatment due to its simple reactor design. In this work, for a system available in the laboratory a hydrodynamic reactor is designed based on literature recommendations. On the designed Venturi tube, two-dimensional numerical simulations were investigated by the means of CFD computations using the commercial software package, Ansys Fluent. The resulting cavitation bubbles were analysed at different inlet pressures.

1. INTRODUCTION

Nowadays the treatment and utilization of the ever-increasing sewage sludge is a major environmental problem. The amount of sewage sludge generated in Hungary is projected to increase from ~179 thousand tons registered in 2013 to ~250 thousand tons by 2027, therefore a unified strategy for efficient treatment and utilization of sewage sludge has been established (Sewage Sludge Management and Recovery Strategy 2014-2023, [1]). Most importantly, sewage sludge should not be considered as waste to be disposed of, but as a secondary raw material for soil fertilising or renewable energy source. This is the main idea of the ongoing research at University of Miskolc [2].

Wastewater and sewage sludge are transformed into micronutrients and macronutrients that are easily absorbed by plants, and their organic matter content improves many soil properties. Wastewater can contain toxic heavy metals, drug residues, which are non-degradable substances that may enter the food chain through uptake or erosion, thereby endangering the environment and human health. Only wastewater stabilized by aerobic, anaerobic, chemical treatment or stored for 3-6 months may be applied to agricultural land. Many new chemical and biological methods have been proposed in the literature, one of these promising new disinfection technologies is the use of cavitation, which has the great advantage of not introducing new chemicals into the water.

Cavitation is a physical phenomenon when the pressure of a liquid is reduced to a pressure of saturated water vapour and a vapour phase appears in the liquid, as so-called cavitation bubbles. When the cavitation bubble collapses, where condensation and vapour compression occur, this energy is released. When the bubble collapses, thousands of kelvin temperatures occur (theoretically), but they last for a very short time (~ 1 μs), during which time the temperature drops to the temperature of the surrounding liquid [3]. These conditions are suitable for breaking the cell wall of the organic material. Through sludge treatment, they increase biodegradability and increase anaerobic digestion, resulting in higher biogas production, less retention time and reduced sludge.

There are two types of cavitation methods: acoustic (ultrasonic) and hydrodynamic cavitation. Acoustic cavitation is induced by the presence of pressure waves that propagate through the liquid region. Acoustic cavitation is most often used for the treatment of industrial wastewater [4-6]. The problem with ultrasonic cavitation devices is that cavitation effects only occur near the vibrating surface, which reduces the ability to treat the entire wastewater. According to Dular et al. (2016) [7], the application of hydrodynamic

cavitation is better because it is easily scaled, it can operate in continuous mode, and in many cases has a higher removal efficiency than acoustic cavitation. For example Patil and Gogate [8] found for the degradation of methyl parathion pesticide that the hydrodynamic cavitation is around 20 times more energy efficient than acustic cavitation

Hydrodynamic reactor designs are typical orifice [9] or Venturi type [10, 11] construction. Many researchers have studied high-speed visualization of cavitation inception and growth through individual Venturi devices [12, 13]. The Venturi volumetric flowmeter consists of a simple design with a convergent, a throat and a divergent section. A fluid's velocity must increase as it passes through a constriction, while its static pressure must decrease in accord with the principle of conservation of mechanical energy (Bernoulli's principle). Thus, any gain in kinetic energy a fluid may attain by its increased velocity through a constriction is balanced by a drop in pressure. If the throttle is high enough, the local absolute pressure drops below the unsaturated vapour pressure and microbubbles appear in the liquid. In the diffuser section of the Venturi tube, velocity decreases and pressure increases. As the pressure increases, the cavities collapse, leading to strong noise, vibration and erosion of the surrounding solid bodies.

The main objective of this work is to design a Venturi tube for hydrodynamic cavitation based in literature and two-dimensional flow through the Venturi is investigated numerically using CFD method. Optimal grid resolution for such a flow were selected by using a preliminary study. Numerical calculations were carried out to analyse cavitating flows and to describe the two-phase flow structures in Venturi geometry.

2. COMPUTATIONAL SETUP

2.1. Geometry design

An experimental equipment is available in the laboratory from which a hydrodynamic reactor is designed according to literature recommendations. The experimental setup consists of an open tank, a centrifugal pump, a pipeline and a discharge point. The working principle of the setup is based on the recirculation of the fluid inside the tank by the centrifugal pump through the cavitation device and refeeding it back to the tank. After specific recirculation time, the content of the tank will be discharged through a discharge point.

The schematic drawing of a Venturi tube is shown in Figure 1. The main structural parameters are the pipe diameter (D), the throat diameter (d), the convergent or inlet angle (α), the throat length (L_{th}), the diffuser or outlet angle (β).
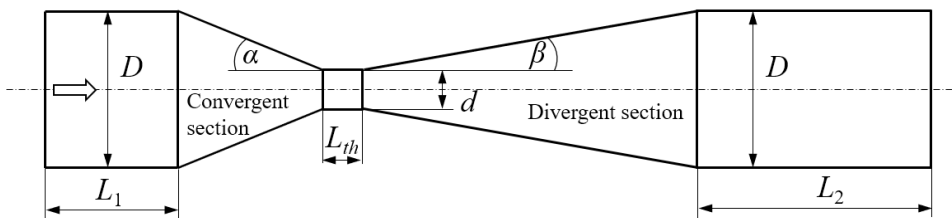

Figure 1. Schematic diagram of the Venturi

The effects of the structural parameters of the Venturi tube, pressure drop and mass flow rate have already been widely investigated. Therefore, when designing the geometry of Venturi, geometric parameters recommended in the literature have been taken into account. Table 1 summarizes some Venturi designations used in the experimental and numerical computations. The literature deals with small Venturi pipes (D=12–60 mm), but our available pipe diameter is 97 mm. Li et al. [11] found two key geometric parameters based on their numerical simulations: the outlet angle, as it strongly affects the pressure profile; and the diameter ratio, as it affects the power consumption. The initial power decreases with the reduction of the diameter ratio, so a small diameter ratio should be chosen.

Simpson and Ranade [10] investigated the influence of two geometric parameters such as the length of Venturi throat and diffuser angle on the inception and extent of cavitation. They suggested an optimum configuration, which offers a minimum power input with a low diffuser angle (β=7.5°) and a low ratio of throat length to diameter (L_{th}/d=1).

Based on literature recommendations, the following parameters are selected: for the Venturi tube diameter (D= 97mm) the diameter ratio is d/D=0.18, the convergent angle is α=22.5°, the length of the throat is equal to the diameter of the throat (L_{th}=d) and the outlet angle is β=7°. The walls of the converging and diverging section are straight. An additional length of 250 mm (L_1) before inlet and L_2=400 mm after outlet is added in the CFD model to obtain a fully developed flow and to avoid any entrance or exit effects.

Table 1 Presents various structural parameters of the Venturi model with other studies

Authors	Method	D [mm]	d [mm]	d/D	L_{th} [mm]	α [°]	β [°]
Abdulaziz [12]	EM	20	3.6	0.18	9	6.2	6.2
Brinkhorst et al. [13]	CFD	25.5	11.2	0.439	11.2	10.5	3.5
Bertoldi et al. [14]	EM	16	4	0.25	3	20	7
Dastane et al. [15]	CFD	20	2	0.1	0	22.61	6.4
Li et al. [11]	CFD	9	2-4.5	0.167-0.5	5; 10; 20	5-45	5-90
Simpson & Ranade [10]	CFD	12	2	0.167	0; 2; 4; 6	22.5	7.5-12.5
Wang [16]	EM	50	16	0.32	16	22.5	5

(CFD – Computational Fluid Dynamics, EM – experimental measurement)

2.2. Numerical solution

In this study two-dimensional, unsteady flow has been carried out using Ansys Fluent commercial software based on the Finite Volume Method (FVM). The FVM is a numerical technique that transforms the partial differential equations representing conservation laws over differential volumes into discrete algebraic equations over finite volumes (or elements or cells). Most researchers [10, 11, 15] recommend the k-ω SST model for modelling cavitation flow, therefore this turbulence model was used. Pressure velocity coupling was solved using SIMPLE algorithm, with the PRESTO! discretization scheme applied for pressure. The First Order Discretization scheme was used for the momentum, turbulent quantities and vapour transport. The numerical simulations were carried out considering a homogeneous mixture of liquid water and water vapour. A mixture model was used to model the cavitation flow, where the liquid is assumed to be incompressible and the slip between the two phases is neglected. The fluid properties are constant.

The flow boundary conditions were defined in terms of inlet pressure and outlet pressure. The inlet pressure values were varied from 1.05 bar to 5 bar, while the outlet was maintained at atmospheric pressure. The walls of the Venturi were considered to have a no-slip condition.

2.3. Mesh independence study

In addition to the implementation of boundary conditions and the quality of the numerical solutions, the grid resolution in the domain is important for the reliability of the numerical results. The solution of the problem should be tested on different grid resolutions and by means of this process, the optimum grid should be determined for the calculations. The computations were performed for four different mesh size with 68k, 97k, 141k, 185k elements. The grid test was performed under the same boundary conditions, where no cavitation flow has yet occurred. Comparison of pressure distribution at the centre of the Venturi and velocity profile at the throat are shown in Fig. 2. It was found that the solution was mesh independent beyond 141k elements, and hence this mesh was used for all further simulations.

3. RESULTS AND DISCUSSION

In the present study, computations for a Venturi flow were carried out at different pressure ratio (P_r=p_{in}/p_{out}, where p_{out} is fix value). In the Venturi the flow oscillated initially and stabilized after some time. The simulation was considered to be completed when the inlet, as well as outlet flows were stabilized and no fluctuations in the flow rate were observed with respect to the flow time. The flow was usually found to stabilize in 0.5–0.7 s.
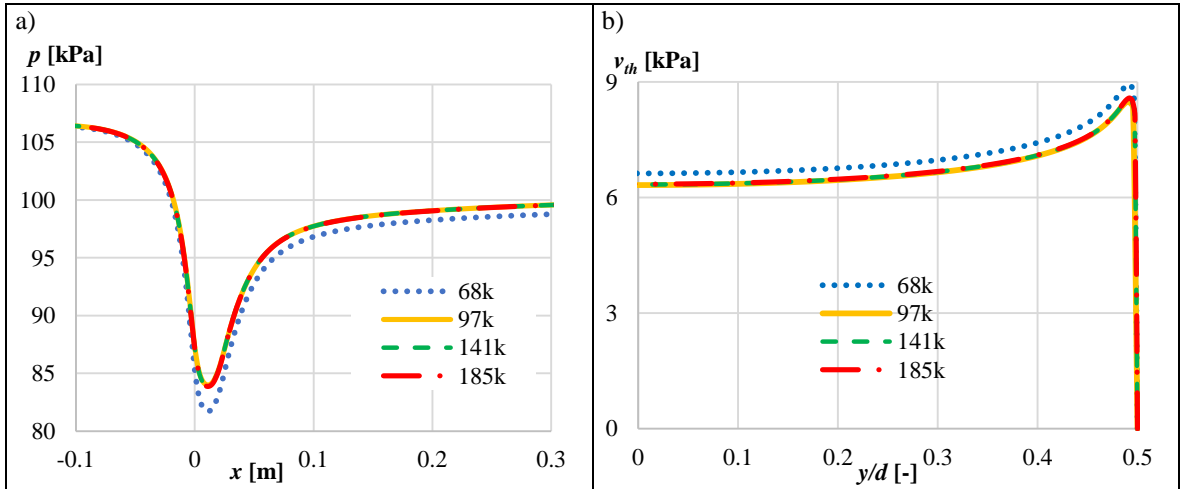

Figure 2. a) Comparison of pressure distribution at centre of the Venturi and b) velocity profile at the throat for different grids

The number of cavity forming in the cavitational reactor and the cavitational zone intensity is largely dependent on operating condition pressure gauge at the inlet and the cavitation number associated with the flow. For characterization of the cavitation is used so-called cavitation number, represented by the formula

$$\sigma = \frac{p_d - p_v}{\frac{1}{2} \cdot \rho \cdot v_{th}^2} \tag{1}$$

where p_d is the downstream pressure, p_v is the vapour pressure, v_{th} is the velocity in the throat, and ρ is the liquid density. The pressure change induced by a Venturi tube is characterized by the loss coefficient (L_c), defined as:

$$L_c = \frac{p_u - p_d}{\frac{1}{2} \cdot \rho \cdot v_{th}^2} \tag{2}$$

where p_u is the upstream pressure.

Fig. 3a shows the loss coefficient with the cavitation number. In the no cavitation section the loss coefficient is a constant value for each geometry, because the pressure loss is proportional to the square power of throat velocity in this region. Once the cavitation inception is reached, the extra loss coefficient induced by cavitation starts to rise linearly as σ further decreases. As seen in the figure, it contains a global description of cavitation behaviour with a clearer indication of inception where L_c curve suddenly change. This change can also be seen in Fig. 3b, which shows the pressure ratio versus the throat velocity.

Distributions of cavitation volume fraction are shown in Fig.4 for different pressure ratio. The cavity length rises with the increase of the pressure rate. It can be seen, that the maximum cavitation volume fraction arises at the tube wall and distribution of cavitation volume fraction is not regular. Abdulaziz's experimental studies [12] had similar results to me. He found that the cavitation inception starts at the lower edge of the throat and the asymmetrical distribution of vapour about the horizontal centreline was observed by increasing the inlet pressure.
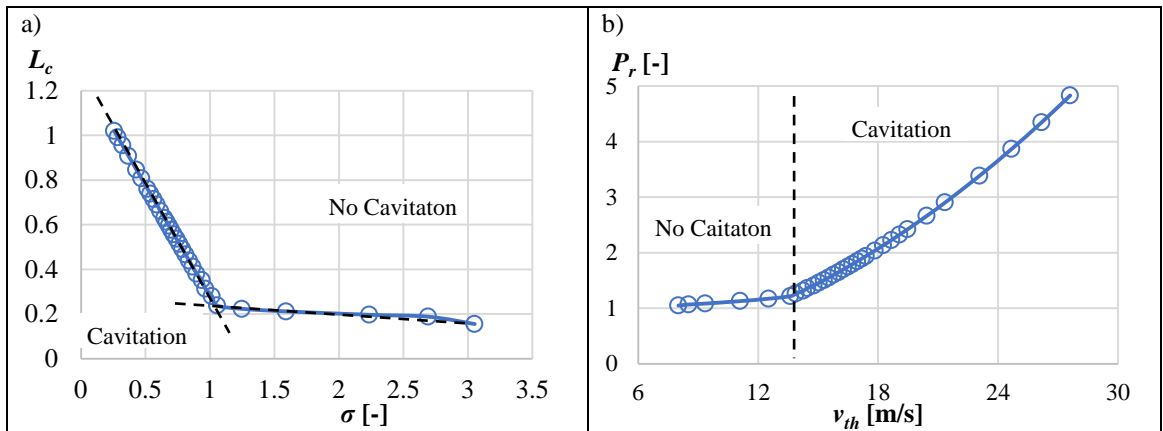

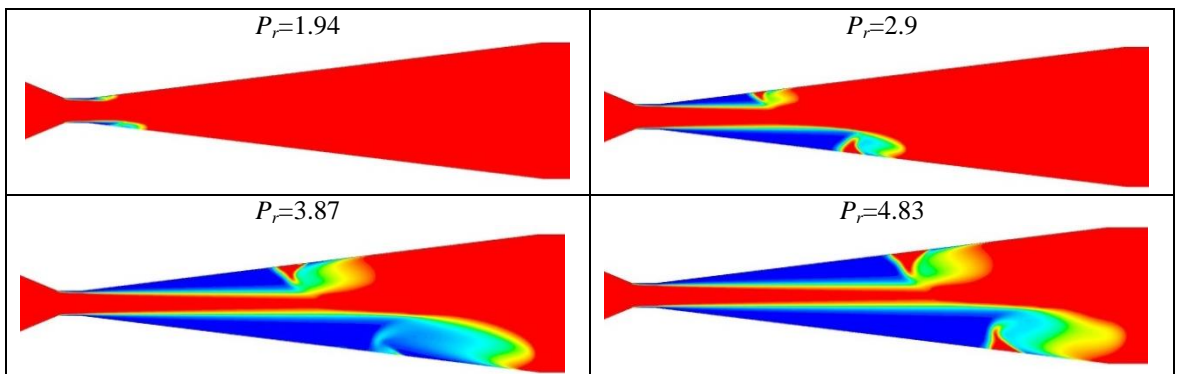*Figure 3. a) The loss coefficient versus cavitation number and b) pressure ratio versus throat velocity*

Figure 4. Phase distribution for different pressure ratio

4. CONCLUSIONS

In the present study, a hydrodynamic reactor, a Venturi tube had designed, based on literature recommendations and it was tested with numerical simulation. The cavitation phenomenon was investigated by flowing through the Venturi and a two-dimensional numerical simulation was performed by using the commercial code of Ansys Fluent. A mixture model based on a water-vapour-phase mixture was used. The cavitation region was analysed for different inlet pressure values. Calculations show that the cavitation zone is asymmetric, which may be due to the three-dimensional turbulent flow, therefore a 3D model is needed for further calculations. As a next step, the effect of the outlet angle decreasing is investigated on the cavitation flow with a 3D model.

ACKNOWLEDGEMENTS

REFERENCES

[1] Strategy 2014 Consortium: Sewage Sludge Management and Recovery Strategy 2014-2023, Hungarian.

[2] Establishing products range from bio raw materials with the special regard to a local technological flowsheet. GINOP-2.2.1-15-2017-00069 R&D Project. Project Leader: Dr. Ljudmilla Bokányi.

[3] Pankaj, M. Ashokkumar, Theoretical and Experimental Sonochemistry Involving Inorganic Systems, Springer 2011, ISBN 978-90-481-3886-9.

[4] P. Braeutigam, M. Franke, B. Ondruschka, Effect of ultrasound amplitude and reaction time on the anaerobic fermentation of chicken manure for biogas production, Biomass and Bioenergy, 63 (2014), pp. 109-113.

[5] S. T. L. Harrison, Bacterial cell disruption: a key unit operation in the recovery of intracellular products, Biotechnology Advances, 9 (1991), pp. 217-240.

[6] K. Nickel, Ultrasonic disintegration of biosolids – benefits, consequences and new strategies, TU Hamburg-Harburg Reports on Sanitary Engineering, 35 (2002), pp. 189-199.

[7] M. Dular, T. Griessler-Bulc, I. Gutierrez-Aguirre, E. Heath, T. Kosjek, A. K. Klemenčič, M. Oder, M. Petkovšek, N. Rački, M. Ravnikar, A. Šarc, B. Širok, M. Zupanc, M. Zitnik, B. Kompare, Use of hydrodynamic cavitation in (waste)water treatment, Ultrasonics Sonochemistry, 29 (2016), pp. 577–588.

[8] P. N. Patil, P. R. Gogate, Degradation of methyl parathion using hydrodynamic cavitation: Effect of operating parameters and intensification using additives, Separation and Purification Technology, 95 (2012), pp. 172–179.

[9] M. N. H. Jusoh, A. Aris, J. Talib: Hydrodynamic cavitation using double orifice- plates for the generation of hydroxyl radicals, Jurnal Teknologi, 78 (11) (2016), pp. 41-47.

[10] A. Simpson, V. V. Ranade, Modeling Hydrodynamic Cavitation in Venturi: Influence of Venturi Configuration on Inception and Extent of Cavitation, AIChE Journal, 65 (1) (2019), pp. 421-433.

[11] M. Li, A. Bussonnière, M. Bronson, Z. Xu, Q. Liu, Study of Venturi tube geometry on the hydrodynamic cavitation for the generation of microbubbles, Minerals Engineering, 132 (2019), pp. 268–274

[12] A. M. Abdulaziz, Performance and image analysis of a cavitating process in a small type venturi, Experimental Thermal and Fluid Science, 53 (2014), pp. 40-48.

[13] S. Brinkhorst, E. von Lavante, G. Wendt, Numerical investigation of cavitating Herschel Venturi-Tubes applied to liquid flow metering, Flow Measurement and Instrumentation, 43 (2015), pp. 23–33.

[14] D. Bertoldi, C.C.S. Dallalba, J. R. Barbosa Jr., Experimental investigation of two-phase flashing flows of a binary mixture of infinite relative volatility in a Venturi tube, Experimental Thermal and Fluid Science, 64 (2015), pp. 152–163.

[15] G. G. Dastane, H. Thakkar, R. Shah, S. Perala, J. Raut, A.B. Pandit, Single and multiphase CFD simulations for designing cavitating venturi, Chemical Engineering Research and Design, 149 (2019), pp. 1–12.

[16] J. Wang, L. Wang, S. Xu, B. Ji, X. Long, Experimental investigation on the cavitation performance in a venturi reactor with special emphasis on the choking flow, Experimental Thermal and Fluid Science, 106 (2019), pp. 215–225.